Dynamic Model Estimation for Power System Areas from Boundary Measurements

Andrija T. Sarić
Dept. of Power, Electronics and Communication Engineering
Faculty of Technical Sciences, University of Novi Sad, Serbia
asaric@uns.ac.rs

Mark K. Transtrum[1] and Aleksandar M. Stanković[2]
[1]Dept. of Physics and Astronomy
[1] Brigham Young University
[2] Dept. of Electrical and Computer Engineering
[2] Tufts University, Medford, MA, USA
[1]mktranstrum@byu.edu; [2] astankov@ece.tufts.edu

***Abstract*—The paper describes a REI-based procedure for estimating parameters of a dynamic model from measurements in the boundary buses/branches. Parameter identification of equivalent synchronous generators in fictitious buses is performed by Weighted Least Square (WLS) nonlinear optimization to minimize the difference between online measurements and transient responses of reduced power system.**

***Index Terms*—Dynamic Equivalent, Online measurement, Parameter Identification, Radial, Equivalent and Independent (REI).**

I. INTRODUCTION

In this paper we describe a procedure for estimating a dynamic equivalent of a power system area from measurements in boundary buses/branches. This problem has attracted the attention of electric energy engineers [1-9] and our work aims to contribute to the literature by proposing a two-step procedure which is a modification of the widely used REI approach [5,6]:

1) static (network) parameters are calculated in a modified REI procedure that uses fixed voltages closer to typical operation;
2) we identify the dynamic parameters from measurements, using a weighted least square procedure (instead of combining *known* parameter sets of different dynamic components).

The outline of the paper is as follows: *Section II* describes the problem setting; *Section III* describes our procedure, *Section IV* contains the results obtained in a multi-machine benchmark example, followed by conclusions in *Section V*.

II. DYNAMIC MODEL FOR PARAMETER IDENTIFICATION

The power system under study is divided into three parts (see Fig. 1): 1) measured part of power system (detailed model), 2) observable transmission network, and 3) non-measured part of power system (to be replaced with a dynamic equivalent). Synchronous generators (SGs) in 'Detailed model' part are modeled by physics-based mathematical equations [10]. Transmission network is modeled by actual topology and branch models (lines, transformers etc.) in the non-reduced part of power system.

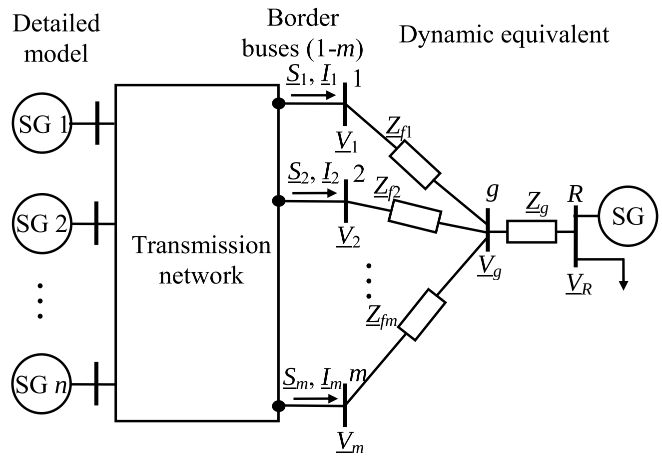

Fig. 1. Main parts of power system model.

Dynamic models of power systems are typically written in differential-algebraic equation (DAE) form:

$$\dot{\boldsymbol{x}} = \boldsymbol{f}(\boldsymbol{x}, \boldsymbol{z}, \boldsymbol{p}, \boldsymbol{u}, t)\,; \tag{1}$$

$$\boldsymbol{0} = \boldsymbol{g}(\boldsymbol{x}, \boldsymbol{z}, \boldsymbol{p}, \boldsymbol{u}, t)\,, \tag{2}$$

where $\boldsymbol{x}$ is the vector of (differential) state variables, $\boldsymbol{z}$ are the algebraic variables, $\boldsymbol{p}$ are parameters, $\boldsymbol{u}$ are inputs (typically assumed to be known in estimation studies) and t is the time variable.

System measurement vector is assumed to be of the form:

$$\boldsymbol{y} = \boldsymbol{h}(\boldsymbol{x}, \boldsymbol{z}, \boldsymbol{p}, \boldsymbol{u}, t)\,. \tag{3}$$

The parameter vector ($\boldsymbol{p}$) is to be estimated from available online measurements ($\boldsymbol{y}$), and there typically exists some prior information about parameters, often in the form of plausible ranges for each. The least-square optimization formulation of the identification problem is by far the most prevalent in the literature.

It turns out that the key quantities in the case of least square identification are parametric sensitivities whose dynamics is described by the following equations:

$$\frac{d}{dt}\frac{\partial \boldsymbol{x}}{\partial \boldsymbol{p}} = \frac{\partial \boldsymbol{f}(\boldsymbol{x},\boldsymbol{z},\boldsymbol{p},\boldsymbol{u},t)}{\partial \boldsymbol{x}} \cdot \frac{\partial \boldsymbol{x}}{\partial \boldsymbol{p}} + \frac{\partial \boldsymbol{f}(\boldsymbol{x},\boldsymbol{z},\boldsymbol{p},\boldsymbol{u},t)}{\partial \boldsymbol{z}} \cdot \frac{\partial \boldsymbol{z}}{\partial \boldsymbol{p}} + \frac{\partial \boldsymbol{f}(\boldsymbol{x},\boldsymbol{z},\boldsymbol{p},\boldsymbol{u},t)}{\partial \boldsymbol{p}}\,; \tag{4}$$

978-1-5090-4168-8/16/$31.00 ©2016 IEEE

$$\mathbf{0}=\frac{\partial \boldsymbol{g}(\boldsymbol{x},\boldsymbol{z},\boldsymbol{p},\boldsymbol{u},t)}{\partial \boldsymbol{x}}\cdot\frac{\partial \boldsymbol{x}}{\partial \boldsymbol{p}}+\frac{\partial \boldsymbol{g}(\boldsymbol{x},\boldsymbol{z},\boldsymbol{p},\boldsymbol{u},t)}{\partial \boldsymbol{z}}\cdot\frac{\partial \boldsymbol{z}}{\partial \boldsymbol{p}}+\frac{\partial \boldsymbol{g}(\boldsymbol{x},\boldsymbol{z},\boldsymbol{p},\boldsymbol{u},t)}{\partial \boldsymbol{p}};\ (5)$$

$$\frac{\partial \boldsymbol{h}}{\partial \boldsymbol{p}}=\frac{\partial \boldsymbol{h}(\boldsymbol{x},\boldsymbol{z},\boldsymbol{p},\boldsymbol{u},t)}{\partial \boldsymbol{x}}\cdot\frac{\partial \boldsymbol{x}}{\partial \boldsymbol{p}}+\frac{\partial \boldsymbol{h}(\boldsymbol{x},\boldsymbol{z},\boldsymbol{p},\boldsymbol{u},t)}{\partial \boldsymbol{z}}\cdot\frac{\partial \boldsymbol{z}}{\partial \boldsymbol{p}}+\frac{\partial \boldsymbol{h}(\boldsymbol{x},\boldsymbol{z},\boldsymbol{p},\boldsymbol{u},t)}{\partial \boldsymbol{p}}.(6)$$

These equations are linear in terms of sensitivities, but the matrices involved do vary along a system trajectory.

III. Parameter Identification of External Dynamic Equivalent

The dynamic equivalent is composed from equivalent REI (Radial, Equivalent and Independent) equivalent branches [5,6] and equivalent SG (see Fig. 1), where recommended equivalent SG dynamic models are outlined in [11, 12].

Parameter identification of dynamic equivalent is performed from available online measurements (in boundary and in-depth points of the transmission network), where it is assumed that all border points are equipped with complete sets of electrical measurements (V_i, θ_i, P_i and Q_i, where $\underline{V}_i = V_i e^{j\theta_i}$ and $\underline{S}_i = P_i + jQ_i$ are measured complex voltage in i-th border bus and complex power flow from i-th bus to external network, respectively – see Fig. 1).

The proposed algorithm can be summarized by the following steps:

Step 1: Initial values of inner ($\underline{Z}_{fi};\quad i=1,\,2,\,\cdots,\,m$) and outer ($\underline{Z}_g$) external fictitious impedances. Two options are recommended and investigated:

a) $\underline{Z}_{fi}=0;\quad i=1,\,2,\,\cdots,\,m$ and $\underline{Z}_g=0$ (these values lead to a minimum loss equivalent).

b) For assumed (initial) values of inner and outer external fictitious bus voltages (for example, $\underline{V}_g=1$ p.u. and $\underline{V}_R=\underline{S}_R/\underline{I}_R^*$; typical assumption for REI equivalent is $\underline{V}_g=0$ [5, 6]; however, we found out that values closer to normal operation result in improved equivalents. Next, we calculate inner and outer external impedances respectively as (see Fig. 1):

$$\underline{Z}_{fi}=\frac{(\underline{V}_i-\underline{V}_g)}{\underline{I}_i};\quad i=1,\,2,\,\cdots,\,m; \qquad (7)$$

$$\underline{Z}_g=\frac{(\underline{V}_g-\underline{V}_R)}{\underline{I}_g}, \qquad (8)$$

where:

$$\underline{I}_i=\frac{\underline{S}_i^*}{\underline{V}_i^*};\quad i=1,\,2,\,\cdots,\,m;$$

$$\underline{I}_g=\underline{I}_R=\sum_{i=1}^{m}\underline{I}_i;$$

$\underline{S}_i=P_i+jQ_i$ ($\underline{I}_i$) is available online measured complex power (current) flow from i-th bus to the external network (fictitious buses).

Step 2: Calculation of inner ($\underline{Z}_{fi};\quad i=1,\,2,\,\cdots,\,m$) and outer ($\underline{Z}_g$) external fictitious impedances (see Fig. 2). There are two characteristic cases:

Case 1: For $\sum_{i=1}^{m}P_i<0$, the external dynamic equivalent is load dominantly (PQ), where P_i is measured active power branch flow from i-th bus to g-th fictitious bus.

Case 2: For $\sum_{i=1}^{m}P_i>0$, the external dynamic equivalent is dominantly a generator (PV).

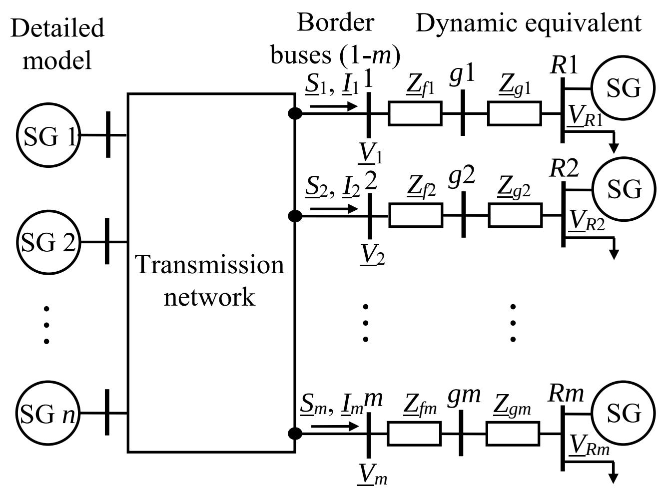

Fig. 2. REI-based fictitious equivalent branches.

For **Case 1** in **Step 2**, inner and outer impedances are determined by the following optimization (to abbreviate the presentation, the equations are written in complex form, while solution is obtained in rectangular coordinates):

$$\hat{\underline{\boldsymbol{Z}}}_{fg}=\min\left\{\frac{1}{2}(V_R^{\mathrm{sp}}-V_R)^2\right\}=\min\left\{\frac{1}{2}[V_R^{\mathrm{sp}}-(V_R+\boldsymbol{J}\underline{\boldsymbol{Z}}_{fg})]^2\right\},(9)$$

where:

$$V_R=\left|\underline{V}_i-\underline{Z}_{fi}\underline{I}_i-\underline{Z}_g\sum_{i=1}^{m}\underline{I}_i\right|;\quad i=1,\,2,\,\cdots,\,m;$$

$$\underline{Z}_{fi}=R_{fi}+jX_{fi};\ \underline{Z}_{Ri}=R_{Ri}+jX_{Ri};$$

$$\underline{\boldsymbol{Z}}_{fg}=\left[\underline{Z}_{f1}\ \cdots\ \underline{Z}_{fm}\ \underline{Z}_g\right]^{\mathrm{T}};$$

$$\boldsymbol{J}=\left[\frac{\partial V_R}{\partial \underline{Z}_{f1}}\ \cdots\ \frac{\partial V_R}{\partial \underline{Z}_{fm}}\ \frac{\partial V_R}{\partial \underline{Z}_g}\right];$$

V_R^{sp} is the specified (requested) voltage in R-buses (for example, 1.0 p.u. for PQ or 1.05 p.u. for PV areas).

Note that Jacobian matrix $\boldsymbol{J}$ in (9) is constant; necessary conditions for optimality in (9) are the "normal equations":

$$\boldsymbol{J}\boldsymbol{J}^{\mathrm{T}}\Delta\underline{\boldsymbol{Z}}_{fg}=\boldsymbol{J}\Delta V_R. \qquad (10)$$

The algorithm is iterated to satisfy $\max\{\Delta V_R\}\le\varepsilon$.

Step 3: Move the impedance $\underline{Z}_g$ to outer external fictitious branches (see Figs. 1 and 2) as:

$$\underline{Z}_{gi} = \underline{Z}_g \frac{\underline{Z}_{fi}}{\sum_{i=1}^{m} \underline{Z}_{fi}}; \quad i = 1,\ 2,\ \cdots,\ m. \tag{11}$$

Step 4: Depending on the **Case** in **Step 2** (PQ vs. PV):

Case 1: For $P_i < 0$, the external equivalent at the end of the REI fictitious equivalent branch is a static load bus (PQ).

Case 2: For $P_i > 0$, the external dynamic equivalent at the end of the REI fictitious equivalent branch is a dynamic generator bus (PV).

Step 5: Calculation of equivalent measurements on fictitious generators from available online measurements in boundary points ($\underline{V}_i$, $\underline{S}_i$; $i = 1,\ 2,\ \cdots,\ m$), as:

$$\underline{S}_{gi} = -\underline{S}_{Ri} = -\left(\underline{S}_i + (\underline{Z}_{fi} + \underline{Z}_{Ri})\left|\underline{I}_i\right|^2\right); \tag{12}$$

$$\underline{V}_{Ri} = \underline{V}_i - (\underline{Z}_{fi} + \underline{Z}_{Ri})\underline{I}_i, \tag{13}$$

where:

$\underline{Z}_{fi} = R_{fi} + \mathrm{j}X_{fi}$; $\underline{Z}_{Ri} = R_{Ri} + \mathrm{j}X_{Ri}$;

$\underline{S}_i = P_i + \mathrm{j}Q_i$ ($\underline{I}_i = \underline{S}_i^* / \underline{V}_i^*$) is available online measured complex power (current) flow from *i*-th bus toward the external network.

Step 6: Calculation of quantities at the end of the REI fictitious equivalent branches (for transient analysis of reduced power system):

Case a: PQ bus:

$$P_{Ri} = P_i + (R_{fi} + R_{Ri})\left|\underline{I}_i\right|^2; \tag{14}$$

$$Q_{Ri} = Q_i + (X_{fi} + X_{Ri})\left|\underline{I}_i\right|^2. \tag{15}$$

Case b: PV bus:

$$P_{Ri} = P_i + (R_{fi} + R_{Ri})\left|\underline{I}_i\right|^2; \tag{16}$$

$$V_{Ri} = \left|\underline{V}_i - (\underline{Z}_{fi} + \underline{Z}_{Ri})\underline{I}_i\right|, \tag{17}$$

where:

$\underline{Z}_{fi} = R_{fi} + \mathrm{j}X_{fi}$; $i = 1,\ 2,\ \cdots,\ m$;

$\underline{Z}_{Ri} = R_{Ri} + \mathrm{j}X_{Ri}$; $i = 1,\ 2,\ \cdots,\ m$;

$\underline{S}_i = P_i + \mathrm{j}Q_i$ ($\underline{I}_i$); $i = 1,\ 2,\ \cdots,\ m$ is complex power (current) flow from *i*-th bus to the external network.

Step 7: Initial parameters of equivalent SG's dynamic model: inertia (H), damping (D), time constants (T_{d0} and T_{q0} in transient and subtransient periods), initial electrical parameters (r_a and reactances x_d and x_q in steady-state, transient and subtransient periods). In our simulations we neglect the exciter and turbine dynamics in fictitious branches (see *Section IV* for additional discussion).

Step 8: Calculation of first partial derivatives of system measurement vector wrt. uncertain parameters $\boldsymbol{J}_{\boldsymbol{p}}(t) = \boldsymbol{J}_{\boldsymbol{p},t} = \partial \boldsymbol{h}(t)/\partial \boldsymbol{p}$; $t = 1,\ 2,\ \cdots,\ T$ (the Jacobian matrix for parameter vector ***p)***.

Step 9: Weighted Least-Square (WLS) fitting of a dynamic equivalent model to experimental data by minimization of the sum of squares of the components of the *N*-dimensional (*N* is number of elements in measurement vector ***h***, where with index ℓ are denoted its components; *T* is number of discrete time steps with current time step denoted by *t*) error (residual) vector $\boldsymbol{r}_t(\boldsymbol{p}) = \boldsymbol{h}_t - \boldsymbol{h}_t(\boldsymbol{p})$ as:

$$\hat{\boldsymbol{p}} = \min\left\{\frac{1}{2}\left\|\sum_{t=1}^{T} \boldsymbol{W}\boldsymbol{r}_t(\boldsymbol{p})\right\|^2\right\} = \min\left\{\frac{1}{2}\sum_{\ell=1}^{N} w_\ell \sum_{t=1}^{T} r_{\ell,t}^2(\boldsymbol{p})\right\}, \tag{18}$$

where ***W*** is diagonal weighting matrix, with values of particular elements discussed in *Section IV*.

Introducing cumulative vectors for analyzed time interval:

$$\boldsymbol{r}(\boldsymbol{p}) = \begin{bmatrix} \boldsymbol{r}_1(\boldsymbol{p}) \\ \boldsymbol{r}_2(\boldsymbol{p}) \\ \vdots \\ \boldsymbol{r}_T(\boldsymbol{p}) \end{bmatrix} = \boldsymbol{h} - \boldsymbol{h}(\boldsymbol{p});\ \boldsymbol{h} = \begin{bmatrix} \boldsymbol{h}_1 \\ \boldsymbol{h}_2 \\ \vdots \\ \boldsymbol{h}_T \end{bmatrix};\ \boldsymbol{h}(\boldsymbol{p}) = \begin{bmatrix} \boldsymbol{h}_1(\boldsymbol{p}) \\ \boldsymbol{h}_2(\boldsymbol{p}) \\ \vdots \\ \boldsymbol{h}_T(\boldsymbol{p}) \end{bmatrix},$$

necessary condition for optimum in (18):

$$\boldsymbol{0} = -\frac{\partial \boldsymbol{h}(\boldsymbol{p})}{\partial \boldsymbol{p}} \boldsymbol{W}[\boldsymbol{h} - \boldsymbol{h}(\boldsymbol{p})] = -\boldsymbol{J}_{\boldsymbol{p}}^{\mathrm{T}} \boldsymbol{W}[\boldsymbol{h} - \boldsymbol{h}(\boldsymbol{p}) - \boldsymbol{J}_{\boldsymbol{p}} \Delta \boldsymbol{p}] \tag{19}$$

provides the system of linear equations for uncertain parameter increments:

$$[\boldsymbol{J}_{\boldsymbol{p}}^{\mathrm{T}} \boldsymbol{W} \boldsymbol{J}_{\boldsymbol{p}}] \Delta \boldsymbol{p} = \boldsymbol{J}_{\boldsymbol{p}}^{\mathrm{T}} \boldsymbol{W}[\boldsymbol{h} - \boldsymbol{h}(\boldsymbol{p})]. \tag{20}$$

Step 10: Check the convergence criterion (ε is a convergence threshold):

$$\max\{\Delta \boldsymbol{p}\} \le \varepsilon. \tag{21}$$

If the convergence criterion is not satisfied replace parameter vector estimate as $\boldsymbol{p} = \boldsymbol{p} + \Delta \boldsymbol{p}$ and continue iterative process with **Step 1b**; otherwise the final parameter estimate is $\hat{\boldsymbol{p}} = \boldsymbol{p}$.

IV. APPLICATION

Our simulations are based on PSAT, a suite of freely available Matlab routines (well documented in [10]) to which we have added our code for the algorithm described in *Section III*.

The IEEE 14-bus test system is composed from [10]:

- 50 state variables: 24 for SGs (two six-order and three four-order models); 20 for exciters (five four-order models), and 6 for turbines (two three-order models).
- 55 algebraic variables: 14×2 bus voltage magnitudes (V) and angles (θ); 5×4 for SGs (P_m, P_g, Q_g and v_f); 5×1 for exciters (v_{fe}); 2×1 for turbines (v_{ft}).

Two different equivalents [**TEST A** (one equivalent SG) and **TEST B** (two equivalent SGs)] were investigated, where only results for **TEST A** are shown (due to the limited space).

Test system is subjected to the three-phase short circuit in bus 1 (see Fig. 3) in *t* = 1.0 s, which cleared after 150 ms.

978-1-5090-4168-8/16/$31.00 ©2016 IEEE

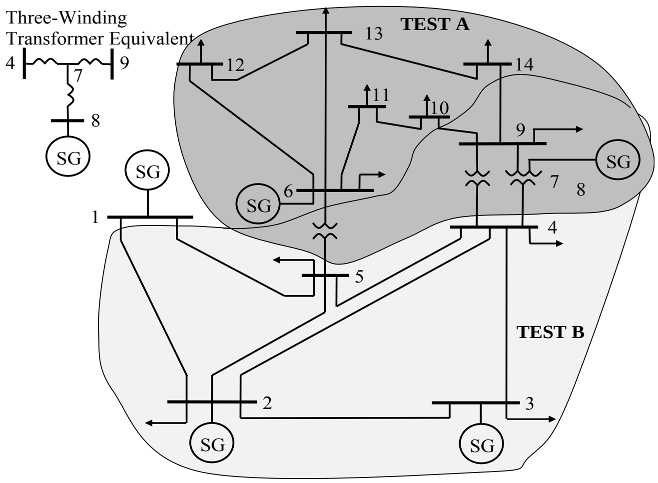

Fig. 3. Single-line diagram of IEEE 14-bus test system with analyzed tests.

For this test example (**TEST A**) the boundary buses are 4 and 5, where 10 online measurements are available: V_4, V_5, θ_4, θ_5, P_{4-7}, P_{4-9}, P_{5-6}, Q_{4-7}, Q_{4-9} and Q_{5-6} (see Fig. 4).

Fictitious impedances calculated in **Steps 2-4** [where requested $V_R^{sp} = 1.02$ p.u. in (9)] are:

- Initial values from **Step 1a**:

  $\underline{Z}_{4-4f} = \underline{Z}_{f,4-4f} + \underline{Z}_{g,4-4f} = (-0.0010 - \mathrm{j}\ 0.0028)\,\text{p.u.}$;

  $\underline{Z}_{5-5f} = \underline{Z}_{f,5-5f} + \underline{Z}_{g,5-5f} = (0.0020 - \mathrm{j}\ 0.0043)\,\text{p.u.}$

- Initial values from **Step 1b** (for $V_g = 1.0$ p.u.):

  $\underline{Z}_{4-4f} = (1.0608 + \mathrm{j}\ 2.3354)\,\text{p.u.}$;

  $\underline{Z}_{5-5f} = (0.1765 - \mathrm{j}0.4081)$ p.u.

Note that our results below are obtained for initial values of fictitious impedances from **Step 1a** (after numerous simulations are concluded that this minimum loss equivalent is preferable for dynamic equivalent parameter identification). Using these values and power flow results we calculate steady-state values and classify of fictitious buses:

- Bus 4*f* (PV): P_{4f} and V_{4f}, calculated as (for power flow results $\underline{V}_4 = (0.9997 - \mathrm{j}0.1729)$ p.u., $P_{4-7} + P_{4-9} = -0.0578$ p.u. and $Q_{4-7} + Q_{4-9} = 0.0288$ p.u.):

  $$\underline{I}_{4-4f} = \frac{(P_{4-7} + P_{4-9} - \mathrm{j}(Q_{4-7} + Q_{4-9}))}{V_4 \mathrm{e}^{-\mathrm{j}\theta_4}} = (-0.0609 - \mathrm{j}0.0183)\ \text{p.u.};$$

  $$\underline{V}_{4f} = \underline{V}_4 - \underline{Z}_{4-4f}\underline{I}_{4-4f} = (0.9997 - \mathrm{j}0.1731)\ \text{p.u.};$$

  $$P_{4f} + \mathrm{j}Q_{4f} = \underline{V}_{4f}\underline{I}^*_{4-4f} = (-0.0578 + \mathrm{j}\ 0.0288)\ \text{p.u.}$$

- Bus 5*f* (PQ): P_{5f}, and Q_{5f}, calculated as (for power flow results $\underline{V}_5 = (1.0083 - \mathrm{j}0.1473)$ p.u., $P_{5-6} = 0.2988$ p.u. and $Q_{5-6} = 0.1110$ p.u.):

  $$\underline{I}_{5-5f} = \frac{(P_{5-6} - \mathrm{j}Q_{5-6})}{V_5 \mathrm{e}^{-\mathrm{j}\theta_5}} = (0.2744 - \mathrm{j}0.1502)\ \text{p.u.};$$

  $$\underline{V}_{5f} = \underline{V}_5 - \underline{Z}_{5-5f}\underline{I}_{5-5f} = (1.0084 - \mathrm{j}0.1458)\ \text{p.u.};$$

  $$P_{5f} + \mathrm{j}Q_{5f} = \underline{V}_{5f}\underline{I}^*_{5-5f} = (0.2987 + \mathrm{j}\ 0.1114)\ \text{p.u.}$$

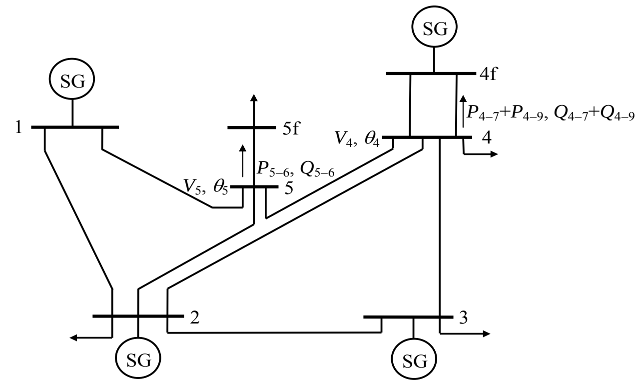

Fig. 4. Reduced IEEE 14-bus test system for **TEST A**.

We thus conclude that the real power flow in branch 4-4f is from the external to the original part of the power system. This means that a SG dynamic model (with uncertain parameters) is connected at bus 4f. For its identification, from the described online measurements and calculated fictitious impedances, a new set of equivalent measurements on SG can be determined: $V_{4f}(t)$, $\theta_{4f}(t)$, $P_{g4f}(t)$ and $Q_{g4f}(t)$. For proposed WLS optimization, in **Steps 8** and **9** we assume that errors in voltage magnitude and SG's active output power are weighted (with diagonal elements $w_\ell = 100000$ – space limitations prevent presentation of a sensitivity analyses to the weighting matrix).

The equivalent SG in the external subsystem is assumed to be described by the six-order dynamic model (see ref. [10] for clarification) without exciter and turbine dynamic models (note that these assumptions gives the conservative results and can be relaxed as needed) and with initial parameters (in corresponding units):

$S_n = 31.3$, $r_a = 0.0041$, $x_d = 1.25$, $x'_d = 0.232$, $x''_d = 0.12$, $T'_{d0} = 4.75$, $T''_{d0} = 0.06$, $x_q = 1.22$, $x'_q = 0.715$, $x''_q = 0.12$, $T'_{q0} = 1.5$, $T''_{q0} = 0.21$, $2H = 10.12$ and $D = 2$.

Previous studies have established that full SG's parameter identification is difficult from typical online measurements [11, 12]. We were investigated following sets of uncertain parameters (mechanical and/or electrical):

Case 1: H, D, x_d, x'_d, x_q and x'_q.

Case 2: x_d, x'_d, x_q and x'_q.

Case 3: H and D.

The estimated SG's parameters obtained by nonlinear WLS-based estimation are shown in Table I, while the detailed results for converged residuals and optimization criterion are shown in Table II. The reduced IEEE 14-bus test system is composed from 36 state variables and 35 algebraic variables, so that the number of state (algebraic) variables is reduced from 50 (55) to 36 (35), or about 28 % (36 %).

In Fig. 5 we compare the original transients (in black) with those produced by the reduced model after parameter estimation – in part a. we show quantities for the equivalent generator inserted in bus 4f (see Fig. 4) and note a satisfactory agreement, and in part b., we show the same quantities for an actual generator (in bus 3) and note excellent agreement.

TABLE I. SG'S OPTIMAL PARAMETER IDENTIFICATION.

	Mechanical parameters		Electrical parameters			
	$2H$	D	x_d	x'_d	x_q	x'_q
Case 1	10.180	2.022	1.723	0.2452	0.4708	0.7271
Case 2	–	–	2.106	0.2148	1.1050	0.7254
Case 3	10.13	2.003	–	–	–	–

TABLE II. RESIDUALS AND OPTIMIZATION CRITERION.

	$\sum_{t=1}^{T} r_{V_t}^2$	$\sum_{t=1}^{T} r_{\theta_t}^2$	$\sum_{t=1}^{T} r_{P_{g,t}}^2$	$\sum_{t=1}^{T} r_{Q_{g,t}}^2$	$\sum_{\ell=1}^{N} w_\ell \sum_{t=1}^{T} r_{\ell,t}^2$
Case 1	0.172	3.005	0.742	1.856	91439.481
Case 2	0.171	3.002	0.711	1.853	88170.027
Case 3	0.163	2.913	0.764	1.884	92655.809

As expected, larger discrepancies are obtained for equivalent fictitious SG (in bus 4f), partly caused by power flow convergence in the 'Equivalent generator (reduced area)' case (the flows involved are very small – about -0.032 p.u. for reactive power). Larger errors in transients appear for reactive/active powers in the same case due to similar reasons (for example, the active power varies between ~0.02 p.u. to ~0.07 p.u.).

The proposed model was tested on a realistic test system (Electric Power Industry of Serbia): 441 buses, 655 branches, 72 SGs (43 of 4-order models and 29 of 6-order models), with exciters and turbines. The model has 850/1314 differential/ algebraic variables. It is interconnected with neighboring countries over ten 400/220 kV lines; 2 lines export energy and are modeled with static (load) equivalents, while 8 lines import energy, modeled with dynamic (SG-based) equivalents. The results are qualitatively very similar and are excluded here due to limited space; we opt for the IEEE 14-bus system that is very familiar to power system analysts.

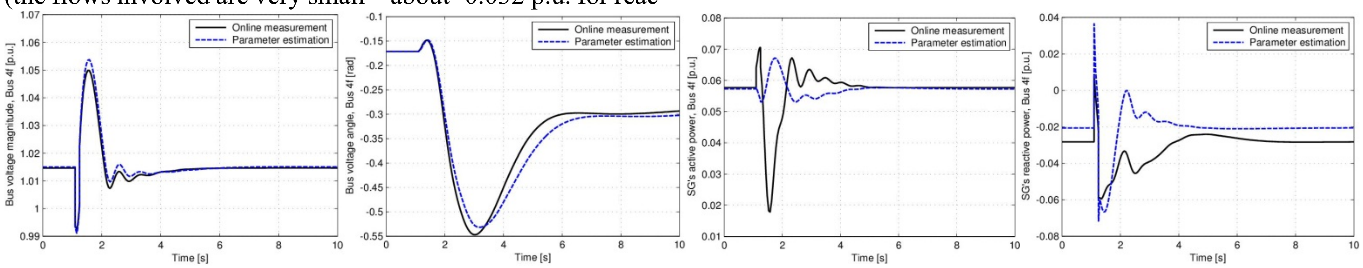

a. Equivalent generator (reduced area).

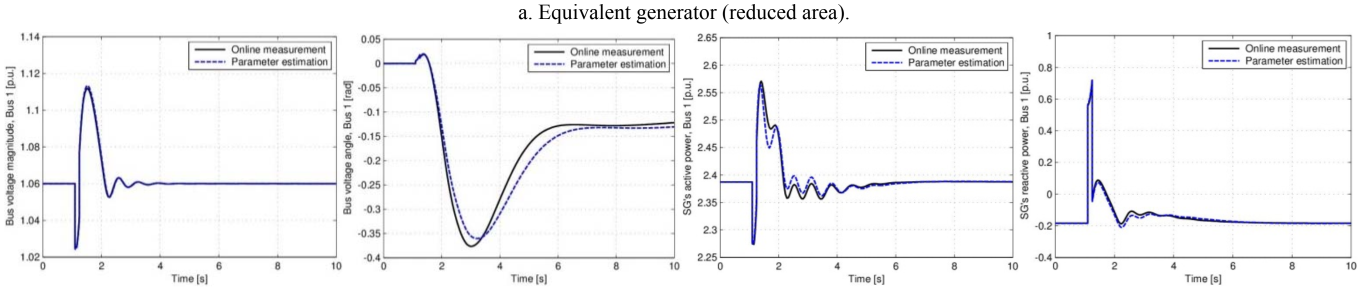

b. Original generator (retained area).

Fig. 5. Transient responses of original and reduced IEEE 14-bus test systems for **TEST A** (**Case 1**).

V. CONCLUSIONS

In this paper we describe a modified REI procedure for estimating a dynamic equivalent of a power system area from measurements in boundary buses. The procedure is illustrated on synchronous generator in a multi-machine benchmark power system, and it is applicable to identification of other dynamical components (e.g., dynamic loads and inverter-connected sources). Advantages of the proposed method include minimal assumed knowledge about the area to be reduced and very promising scaling properties (depending only on measurements); potential downsides include neglected dynamics of exciters and turbines, and measurement availability.

REFERENCES

[1] M.A. El-Sharkawi, "Choice of model and topology for external equivalent systems," *IEEE Trans. on Power Apparatus and Systems*, vol. 20, no. 12, pp. 3761-3768, Dec. 1983.

[2] X. Lei, D. Povh, O. Ruhle, "Industrial approaches for dynamic equivalents of large power systems," *IEEE PES Winter Meeting*, pp. 1036-1042, 2002.

[3] P. Ju, L.Q. Ni, F.Wu, "Dynamic equivalents of power systems with online measurements. Part 1: theory," *IEE Proc.-Gener. Transm. Distrib.,* vol. 151, no. 2, pp. 175-178, Mar. 2004.

[4] M.L. Ourari, L-A. Dessaint, V.-Q. Do, "Dynamic equivalent modeling of large power systems using structure preservation technique," *IEEE Trans. on Power Systems*, vol. 21, no. 3, pp. 1284-1295, Aug. 2006.

[5] M. Gavrilas, O. Ivanov, G. Gavrilas, "REI equivalent design for electric power systems with genetic algorithms," *WSEAS Trans. Circuits & Systems*, vol. 7, no. 10, pp. 911-921, Oct. 2008.

[6] F. Milano, K. Srivastava, "Dynamic REI equivalents for short circuit and transient stability analyses," *Electric Power Systems Research*, vol. 79, no. 6, pp. 878-887, Jun. 2009.

[7] F. Ma, V. Vittal, "Right-sized power system dynamic equivalents for power system operation," *IEEE Trans. on Power Systems*, vol. 26, no. 4, pp. 1998-2005, Nov. 2011.

[8] IEEE PES General Systems Subcommittee - Task Force on Dynamic System Equivalents, "Dynamic system equivalents: A survey of available techniques," *IEEE Trans. on Power Delivery*, vol. 27, no. 1, pp. 411-420, Jan. 2012.

[9] T.N. Preda, K. Uhlen, D.E. Nordgård, T. Toftevaag, "External grid representation for assessing fault ride through capabilities of distributed generation units," *3rd IEEE PES Innovative Smart Grid Technologies Europe (ISGT Europe),* Berlin, Germany, 2012.

[10] F. Milano, *Power System Modeling and Scripting*, Springer, 2010.

[11] M. Burth, G.C. Verghese, M. Velez-Reyes, "Subset selection for improved parameter estimation in on-line identification of a synchronous generator," *IEEE Trans. on Power Systems*, vol. 14, no. 1, pp. 218-225, Feb 1999.

[12] I.A. Hiskens, "Nonlinear dynamic model evaluation from disturbance measurement," *IEEE Trans. on Power Systems*, vol. 16, no. 4, pp. 702-710, Nov. 2001.